THE JOURNAL OF BIOLOGICAL CHEMISTRY Vol. 275, No. 42, Issue of October 20, pp. 32906–32910, 2000
Printed in U.S.A.

Clastogenic Effect of the Human T-cell Leukemia Virus Type I Tax Oncoprotein Correlates with Unstabilized DNA Breaks*

Received for publication, August 10, 2000
Published, JBC Papers in Press, August 31, 2000, DOI 10.1074/jbc.C000538200

Franca Majone‡§ and Kuan-Teh Jeang

From the ‡Department of Biology, University of Padova, Padova 35131 Italy and the Laboratory of Molecular Microbiology, NIAID, National Institutes of Health, Bethesda, Maryland 20892

Expression of the human T-cell leukemia virus type I (HTLV-I) Tax oncoprotein rapidly engenders DNA damage as reflected in a significant increase of micronuclei (MN) in cells. To understand better this phenomenon, we have investigated the DNA content of MN induced by Tax. Using an approach that we termed FISHI, fluorescent in situ hybridization and incorporation, we attempted to characterize MN with centric or acentric DNA fragments for the presence or absence of free 3′-OH ends. Free 3′-OH ends were defined as those ends accessible to *in situ* addition of digoxigenin-dUTP using terminal deoxynucleotidyl transferase. MN were also assessed for centromeric sequences using standard fluorescent in situ hybridization (FISH). Combining these results, we determined that Tax oncoprotein increased the frequency of MN containing centric DNA with free 3′-OH and decreased the frequency of MN containing DNA fragments that had incorporation-inaccessible 3′-ends. Recently, it has been suggested that intracellular DNA breaks without detectable 3′-OH ends are stabilized by the protective addition of telomeric caps, while breaks with freely detectable 3′-OH are uncapped and are labile to degradation, incomplete replication, and loss during cell division. Accordingly, based on increased detection of free 3′-OH-containing DNA fragments, we concluded that HTLV-I Tax interferes with protective cellular mechanism(s) used normally for stabilizing DNA breaks.

It remains incompletely understood as to what are the minimal requirements needed to transform a mammalian cell (1). Despite this, it suffices to say that salient hallmarks of cancer cells include genetic and phenotypic instability. Hence, not surprisingly, it has been suggested that human tumors may contain 100,000 or more mutations (2) with genomic instability in cancers arising from two broad mechanisms: loss of mismatch repair function and infidelity of chromosomal segregation (reviewed in Ref. 3). In view of the link between mutations and cancers, it is attractive to consider that perhaps transforming viruses exert pathology through increasing cellular mutability.

Human T-cell leukemia virus type I (HTLV-I)[1] and the leukemia engendered by this virus, adult T-cell leukemia (ATL), describe an important model system for studying human cancers. ATL cells are well known for heightened burden of damaged DNA (reviewed in Ref. 4). Previously, we have implicated the HTLV-I-encoded oncoprotein, Tax, in cellular DNA damage by correlating increased formation of micronuclei (MN) in cells (5, 6) with the synthesis of this viral protein.

MN are small nuclei-like bodies found outside the main nucleus produced as consequences of chromosomal damage (7, 8). They exist at a low prevalence in cells ambiently and can be induced *ex vivo* by genotoxic compounds with different mechanisms of action. Aneuploidogenic agents produce MN with whole chromosomes or centric chromosomal fragments, while clastogenic compounds induce MN that contain acentric fragments (8). MN induced by HTLV-I Tax was previously verified by fluorescent stainings with human antikinetochore antibodies (5) to contain both aneuploidogenic (*i.e.* kinetochore(+)) and clastogenic (*i.e.* kinetochore(−)) changes (5). One interpretation of these results is that this viral oncoprotein affects both the mismatch repair (clastogenic) and the fidelity of chromosomal segregation (aneuploidogenic) functions postulated to be deficient in human cancers. Mechanistically, the aneuploidogenic effect of Tax was recently proposed to stem from its abrogation in cells of a human mitotic spindle assembly checkpoint (9). As yet, the clastogenic effect of Tax remains molecularly unexplained.

In yeast, several proteins, such as yKu (10) and SIR (11), have recently been shown to associate with telomeric TG-rich repeats. These proteins serve to protect the termini of eukaryotic chromosomes from degradation and end-end fusion. Ku and SIR proteins can be released from telomeres and be recruited rapidly to new breaks in chromosomes, suggesting a role for these proteins also in the stabilization and preservation of DNA ends generated by unexpected (and perhaps exogenously induced) cleavages (11, 12). Indeed, yeast strains deficient for yKu and SIR proteins are hypersensitive to clastogenic agents (11, 12). One corollary of these observations is that termini of new breaks unprotected by telomeres with associated Ku, SIR, and/or other factors are labile. Such ends may not be efficiently repaired and may progress to larger lesions ultimately resulting in gross chromosomal aberrations which could provide the initiating basis for transformation (3).

To explain its clastogenic effect, we asked here whether DNA breaks found in the presence of Tax exist with unprotected (free 3′-OH) or telomere-capped ends. Using *in situ* cytogenetic techniques (FISH and FISHI) and probes specific for centromeres or telomeres (13, 14), we have characterized the nature of

* The costs of publication of this article were defrayed in part by the payment of page charges. This article must therefore be hereby marked "*advertisement*" in accordance with 18 U.S.C. Section 1734 solely to indicate this fact.

§ To whom correspondence should be addressed: Dept. of Biology, Viale G. Colombo 3, 35131 Padova, Italy. Tel.: 39-49-827-6290; Fax: 39-49-827-6280; E-mail: majone@civ.bio.unipd.it.

[1] The abbreviations used are: HTLV-I, human T-cell leukemia virus type I; ATL, adult T-cell leukemia; MN, micronuclei; FISH, fluorescent in situ hybridization; FISHI, fluorescent in situ hybridization and incorporation; DIG, digoxigenin; FITC, fluorescein isothiocyanate; TRITC, tetramethylrhodamine B isothiocyanate; DAPI, 4,6-diamidino-2-phenylindole; Tdt, terminal deoxynucleotidyltransferase enzyme; Cen, centromeric); Te, telomeric; TI, TdT-accessible incorporation.

damaged DNA in Tax-expressing cells. Our finding that Tax disproportionately induces unprotected (free 3′-OH) DNA ends provides a molecular explanation for the clastogenic effect of this oncoprotein.

MATERIALS AND METHODS

Cell Cultures—HeLa cells were cultured as monolayers in Dulbecco's minimal essential medium (Life Technologies, Inc.) supplemented with 10% fetal calf serum (Life Technologies, Inc.) and were maintained in a humidified 5% CO_2 atmosphere at 37 °C. Suspension T-cells were maintained in RPMI 1640 with 10% fetal calf serum.

Micronuclei Assay—For MN assay, suspensions of cells were prepared by trypsinization of log-phase culture of a HeLa clone permanently transfected with a cytomegalovirus-Tax-expressing plasmid. Cells were divided into 40-mm dishes with each dish receiving 8×10^5 cells in 10 ml of medium. The cells were collected 48 h later by trypsinization and were washed in phosphate-buffered saline and fixed in Carnoy's fixative (methanol/acetic acid 3:1, v/v) for 15 min. Interphase preparations were obtained following the procedures described previously (7, 8).

FISH to Detect Centromeres and Telomeres—Centromeric probe (5′-TTG AGG CCC TTC GTT GGA AAC GGG AAT ATC TTG AGG CCC TTC GTT GGA AAC GGG AAT ATC; Ref. 13) was synthesized and labeled with DIG-dUTP. Telomeric probe was either purchased commercially (Oncor) or synthesized as six repetitive copies of the 5′-TTAGGG-3′ hexamers in sense or antisense orientations. Two-color FISH was applied to detect simultaneously centromeric and telomeric DNA sequences in interphase preparations of HeLa cells. Cells cultured on slides were fixed in 70% formamide in 2× SSC (20× SSC = 0.3 M trisodium citrate dihydrate and 3 M NaCl) at 70 °C for 2 min. The samples were then chilled in 70% ethanol at −20 °C. After dehydration and air drying, 30 μl of denaturated (heated at 70 °C for 5 min) hybridization mixture (50% formamide in 2× SSC) containing 2 ng/μl DIG-labeled probe were layered onto each slide. Coverslips were applied and sealed with rubber cement, and hybridization was carried out for 16 h at 37 °C in a moist chamber. Afterward, the slides were washed in 50% formamide in 2× SSC at 43 °C (15 min) and then in 2× SSC at 37 °C (8 min) followed by brief washing in TNT (0.1M Tris-HCl, 0.15 M NaCl, pH 7.5, 0.05% Tween 20) and treatment with 100 μl of TNB (0.1 M Tris-HCl, 0.15 M NaCl, pH 7.5, 0.5% blocking reagent; Roche Molecular Biochemicals, Milan, Italy) for 30 min at 37 °C to prevent nonspecific antibody binding. After coverslip removal, DIG-labeled sequences were detected using a fluorescence-based amplification of signal. This was achieved by incubation with mouse monoclonal anti-DIG antibody (0.5 μg/ml), DIG-conjugated sheep anti-mouse antibody (Roche Molecular Biochemicals, 2 μg/ml) and FITC-conjugated sheep anti-DIG antibody (Roche Molecular Biochemicals, 2 μg/ml). Final 3 × 5-min washes with TNT were followed by dehydration of the slides with ethanol. Slides were counterstained with 0.5 μg/ml propidium iodide in an antifade solution and visualized using wavelength-specific filters (Zeiss, filter set 25). DIG-labeled centromeric DNA sequences (15 ng) and biotinylated telomeric DNA probe (15 ng) were simultaneously hybridized to interphase spreads. The DIG-labeled centromeric probe was detected with TRITC (*red*) following the amplification procedure described above. The biotinylated telomeric probe was labeled with FITC (green) by incubation with FITC-conjugated avidin (Sigma, Milan, Italy) and up to three rounds of amplification by biotinylated anti-avidin (Oncor). Nuclei and micronuclei were counterstained using DAPI (blue) in an antifade solution and viewed through specific filter (Zeiss, filter set 25). The three fluorescent dyes (FITC, TRITC, and DAPI) could be simultaneously viewed and photographed through a triple bandpass filter (Zeiss, filter set 25). Photographs of nuclei and micronuclei were taken on Kodak P 1600 color slide film (5–10-s exposure) on a Zeiss Axiosce microscope using a 100 × 1.3 n.a. objective. For each hybridization, more than 3000 samplings were scored.

FISHI—FISHI detects simultaneously a DNA probe (visualized by standard FISH) and the presence of free 3′-OH DNA ends (visualized by *in situ* incorporation of DIG-dUTP). We used a biotinylated centromeric DNA probe, an oligomeric DNA probe labeled with biotin, and terminal deoxynucleotidyltransferase enzyme. For some experiments, the 3′-end of the probe was blocked with cordycepin (3′-deoxyadenosine). FISHI was performed as described above for FISH up to the post-hybridization wash steps. At that point, the slides were washed in PBD (phosphate-buffered detergent, Oncor) and were then treated for *in situ* incorporation using terminal deoxynucleotidyltransferase enzyme (TdT). As substrates for TdT, DIG-11-dUTP, and DIG-dATP were used. This incorporation reaction contained the following: 10 μl of a buffer with 1 M potassium cacodylate (Roche Molecular Biochemicals), 125 mM Tris-HCl, pH 6.6 (4 °C), 1.25 μg/ml bovine serum albumin, 10 mM $CoCl_2$; 0.2 μl of a solution (Roche Molecular Biochemicals) containing TdT (25 units/μl), 1 mM EDTA, 4 mM 2-mercaptoethanol, 50% glycerol (v/v), pH 6.6 (4 °C); 1 μl of DIG-11-dUTP (1 mM) mixture (Roche Molecular Biochemicals) and 38 μl of distilled water to a final volume of 50 μl. Cells were incubated in this reaction buffer at 37 °C for 1 h in a Hepes-buffered saline moist environment. Then the slides were treated with Hepes-buffered saline containing 0.1% Triton X-100, and 0.5% bovine serum albumin visualization of DIG-dUTP was obtained by incubation (30 min at room temperature) with anti-DIG antibody (1:50) labeled with FITC (Roche Molecular Biochemicals). Finally 3 × 5-min washes with 0.1% Triton and 0.5% bovine serum albumin in Hepes-buffered saline were performed. Visualization of biotinylated centromeric DNA probe was obtained by incubation with Texas Red-conjugated avidin (Sigma) followed by three rounds of amplification using biotinylated anti-avidin (Oncor). Slides were counterstained with DAPI in an antifade solution and photographed through specific filters. For each data point, over 3000 samplings were counted; all points were replicated in at least two independent experiments. Statistical analyses on the frequencies of cytogenetic effects between control, and cells expressing Tax were quantitated using the G test (15).

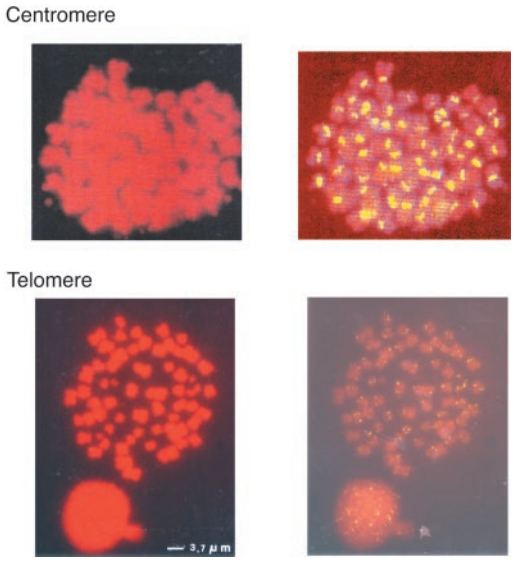

FIG. 1. ***In situ* characterization of centromeric and telomeric probes.** *Top*, metaphase chromosomes of HeLa cells after FISH with a centromeric DNA probe (αCEN-B) labeled with DIG-dUTP were counterstained with propidium iodide (0.3 μg/ml); *left*, visualization of propidium iodide; *right*, fluorescent visualization of centromeric probe (*yellow*). *Bottom*, metaphase HeLa cells stained with propidium iodide and processed for FISH with a telomeric DNA probe; *left*, visualization of propidium iodide; *right*, fluorescent visualization of telomeric signals (dots at the ends of chromosomes).

RESULTS AND DISCUSSION

Characterization of Centromere- and Telomere-specific Probes—To characterize the nature of DNA damage induced by Tax (*i.e.* centric, acentric, telomeric, nontelomeric fragments), we first assessed probes to be used in FISH. Fig. 1 (*top*) shows HeLa cells in metaphase stained with propidium iodide (*left*) followed by FISH with a centromere-specific oligonucleotide (*right*). The DNA probe contained alphoid sequences, which specifically recognize the centromeres of human and mouse chromosomes (13). Hybridization by probe was expected to produce a signal for every chromosome, and indeed the visualized signals were located at precise positions expected for centromeres (Fig. 1, *top right*). Next, we verified our telomere probe. Consistent with that previously reported (14), the telomere probe provided two clearly unambiguous telomeric signals for virtually all chromosomes (98% of expected telomeres were identified; Fig. 1, *bottom right*).

FISHI of Cells—FISH can reveal whether damaged DNA contains/lacks centromeres and/or telomeres. In addition to

this information, we wanted to understand more about the state of DNA breaks in Tax-associated MN. Recent findings in eukaryotic systems (11, 12, 16–19) suggest that a normal response by cells to *de novo* DNA strand breakages is to stabilize breaks by the addition of a telomeric cap, which contains both telomere repeats and telomere-associated proteins. Telomeric capping could be envisioned as a first step in the repair process, protecting new breaks from further instabilities and progressive enlargements. Based on previous knowledge of clastogenic damage produced by Tax (5, 6), we surmised that this oncoprotein could subvert the protective telomeric capping mechanism.

To address the above hypothesis, we asked whether it could be determined if DNA breaks are/are not capped. We reasoned that capped ends might be relatively refractory to incorporation of DIG-dUTP by TdT, while noncapped ends would be more accessible. If one could couple incorporation of DIG-dUTP with standard FISH analysis (*i.e.* FISHI), potentially one could define whether DNA fragments are centric, acentric, telomere-containing, or telomere-free, as well as whether the broken ends might be capped or uncapped. Currently, to our knowledge, simultaneous visualization of FISH with TdT end incorporation (*i.e.* FISHI) has not been done. To establish conditions for FISHI, a biotin-dUTP-labeled probe for detecting acrocentric chromosomes was hybridized to metaphase HeLa nucleus (Fig. 2*B*). The same nucleus was then subjected to DIG-dUTP incorporation using TdT (Fig. 2*C*) to label free 3′-OH associated with the ends of the hybridized probes (see schematic, Fig. 2, *top*). A merged visualization of probe-specific signal with DIG-specific signal showed tight co-localization (Fig. 2*D*), verifying that FISHI technique (TdT incorporation performed simultaneously with FISH) could indeed specifically identify free 3′-OH DNA ends.

More than the ability to detect 3′-OH ends associated with probes used for FISH, our goal was to visualize intrachromosomal breaks with accessible 3′-OH. To distinguish probe-associated from intrachromosomal TdT signals, we next "sealed" each hybridizing oligonucleotide with one molecule of cordycepin (3′-deoxyadenosine) at its 3′-end. The presence of an H instead of an OH group in cordycepin effectively eliminates incorporation at the 3′-ends of probes. Hence, TdT-mediated incorporation of DIG-dUTP, if any, would occur elsewhere, presumptively at damaged cellular DNA with free 3′-OH (Fig. 3, *top schematic*). Accordingly, we performed FISHI using cordycepin-sealed biotin-labeled centromeric DNA probe on interphase HeLa nuclei (Fig. 3). Here, incorporated DIG-dUTP appeared as green spots, while centromeric probe signal was yellow. Consistent with the inability of cordycepin probes to incorporate DIG-dUTP, the green and yellow signals did not overlap (Fig. 3*B*). These results established an ability to characterize intracellular DNA by FISH and TdT end incorporation (FISHI) simultaneously.

We next ascertained that our TdT-mediated DIG-dUTP incorporation assay could quantitatively reflect intracellular DNA breaks. Treatment of cells with clastogenic agents should produce strand breakages, which should correlate with increased signals from TdT incorporation. We incubated HeLa cells with mitomycin C, an inter-/intrastrand cross-linking agent known to cause DNA breaks (20). Compared with mock-treated cells (Fig. 4*A*), treatment with 0.1 μM mitomycin C for 24 h led to a 10–20-fold increase in TdT-mediated signals (Fig. 4*B*), providing a correlation between expected increase in strand breakages with heightened DIG-dUTP incorporation.

Characterization of DNA Damage in Tax-expressing Epithelial and Lymphoid Cells—The above conditions established for FISH and FISHI afforded us techniques to analyze better Tax-induced DNA damage. Previously, we had used transiently transfected cells to study DNA damage (5, 6). However, in such approach, efficiency of transfection could not be higher than

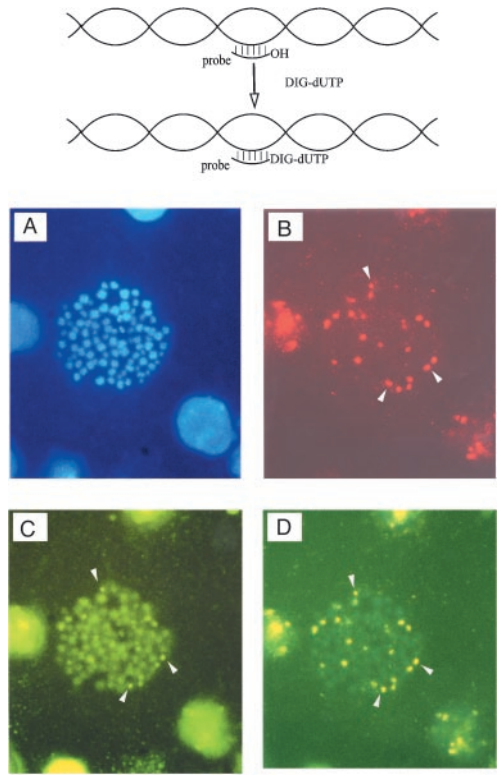

FIG. 2. **Verification of FISHI technique.** A biotin dUTP-labeled probe to detect acrocentric chromosomes coupled with DIG-dUTP incorporation using terminal transferase to detect 3′-OH DNA free ends was used on metaphase HeLa cells. *Top*, schematic representation of the detection procedure. Fluorescent labeled probe is expected to hybridize in a sequence-specific manner to chromosomes. The free 3′-OH end of the probe can then be additionally detected by terminal transferase-mediated incorporation of DIG-dUTP. Presence of the DIG moiety can be visualized independently. *A*, staining of the metaphase cell by DAPI. *B*, the same cell after sequence-specific hybridization of probe and visualization of the probe by avidin Texas Red conjugate (*red* fluorescence). *C*, *in situ* terminal transferase-mediated incorporation of DIG-dUTP and visualization by anti-DIG antibody labeled with FITC (*green* fluorescence). *D*, merged image using a specific filter of the signals from *B* and *C*. Since the acrocentric centromeric probe has a free 3′-OH end, one can observe an overlap between the signal from the biotin-labeled probe (*B*) and the signal from the *in situ* incorporated DIG-dUTP (*C*). *White arrowheads* serve as reference points.

10–20% of all cells (5, 6). To more reproducibly assess effects, we created a HeLa-Tax cell line, using neomycin resistance co-selection, which constitutively expresses an integrated cytomegalovirus-Tax gene (data not shown). Consistent with our previous findings (5), the selected HeLa-Tax cells had a 6–10% increased prevalence of MN over parental HeLa cells (data not shown).

MN from HeLa-Tax and ambient MN from HeLa cells were assessed for the nature of their DNA content. By definition MN contain damaged DNA. We surveyed MN for the presence of centromeric (Cen), telomeric (Te), and TdT-accessible incorporation (TI) of DIG-dUTP. Fig. 5*A* shows that approximately 25% of Tax-induced MN contained centromeric and telomeric signals (Cen(+)Te(+)), indicating with high probability the presence in MN of an intact whole chromosome (*group 1*). This fraction was not significantly different from that observed for control cells (*C*, Fig. 5*A*). Additionally, in Tax-expressing cells, the fraction of MN without centromeric and telomeric (Cen(−)Te(−); Fig. 5*A*, *group 4*) signals, which likely represents acentric interstitial fragments, was also insignificantly different from that for control cells. Based on these results, we concluded that neither MN containing complete chromosomes (*e.g.* Cen(+)Te(+)) nor MN with acentric interstitial fragments (Cen(−)Te(−)) are Tax-specific consequences in HeLa cells. On

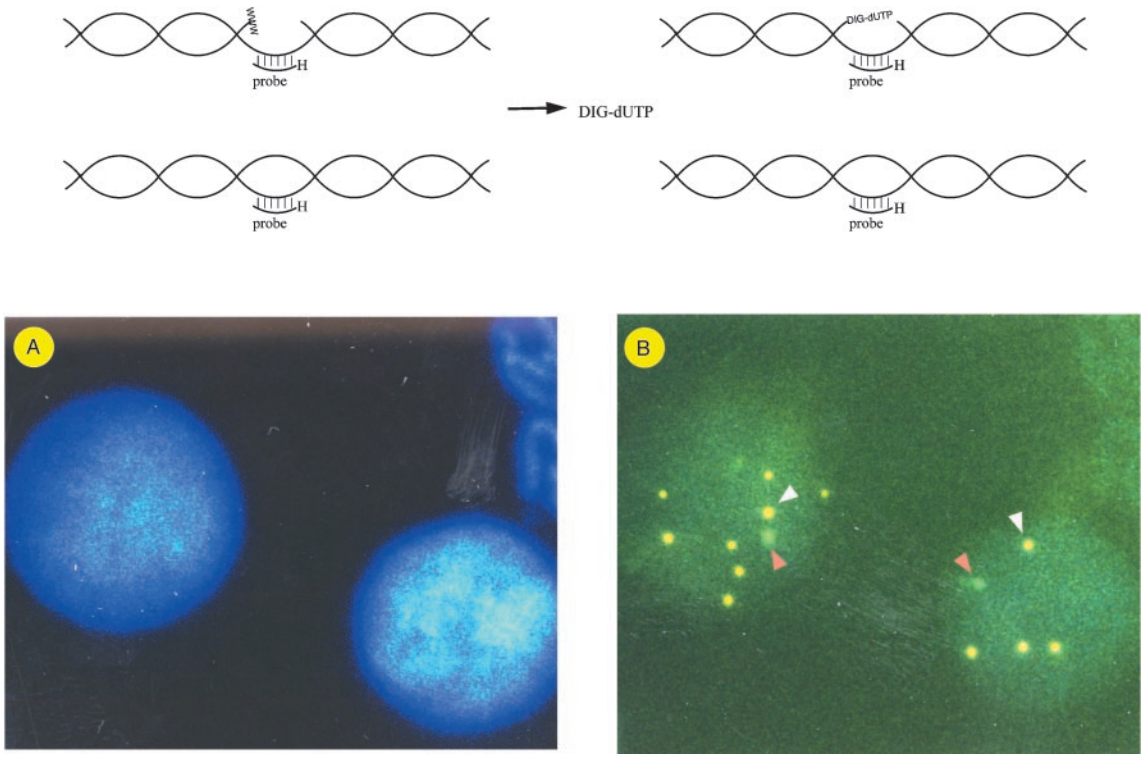

FIG. 3. **FISHI technique using a centromeric biotin-labeled DNA probe on nuclei of interphase HeLa cells.** The probe was constructed to have one molecule of cordycepin (3′-deoxyadenosine) at its 3′-end. An H instead of an OH group in cordycepin at the 3′-end of the probe effectively prevents further incorporation to this end and ensures that terminal transferase-mediated incorporation of DIG-dUTP takes place elsewhere, presumably at damaged cellular DNA ends with free 3′-OH. *Top*, diagrammatic representation of the incorporation schema. *A*, DAPI-stained nuclei. *B*, visualization of the same nuclei after probe hybridization and terminal transferase-mediated incorporation of DIG-dUTP. DIG signal is *green*, and centromeric probe signal is *yellow*. Consistent with the inability of cordycepin-capped probes to incorporate DIG-dUTP, the *green* and *yellow* signals do not overlap. *Open* and *filled arrowheads* point to *yellow* and *green* spots, respectively.

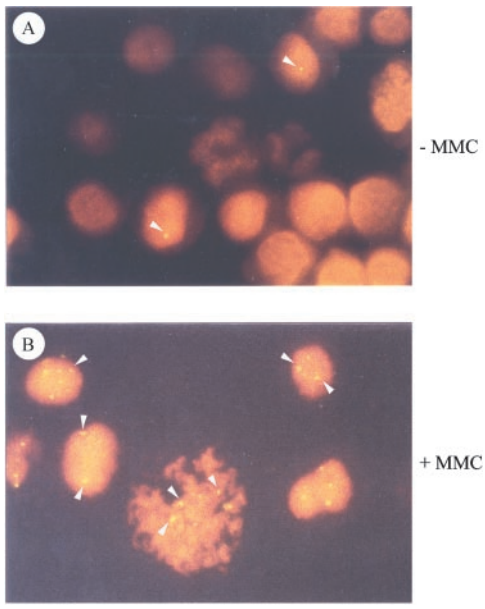

FIG. 4. **DIG-dUTP incorporation is increased after treatment of cells with DNA-damaging agent mitomycin C (*MMC*).** *A*, ambient (−*MMC*) DIG-dUTP incorporation in HeLa cells. *B*, DIG-dUTP incorporation after treatment with 0.1 μM mitomycin C (+*MMC*) for 24 h. *Arrowheads* point to examples of incorporated DIG-dUTP.

the other hand, Tax-expressing cells, compared with controls, had significantly higher frequency of Cen(+)Te(−) MN (Fig. 5A, *group 2*). Hence, under these experimental conditions, the aneuploidogenic effects of Tax (9) are largely restricted to centric fragments of chromosomes and not to intact chromosomes, since the fraction of Cen(+)Te(+) MN was not substantially different in Tax-expressing *versus* control cells (Fig. 5*A*, *group 1*). Last, the type of DNA damage described by telomere-only MN (Cen(−)Te(+); Fig. 5*A*, *group 3*) was significantly less frequent in Tax-expressing cells. These MN can contain either the natural end(s) of a chromosome or an interstitial fragment which has been "repaired" by telomeric capping. The latter would be consistent with the model that eukaryotic chromosomal breaks are "healed" by the addition of telomeric repeats (11, 12, 16–19) with "telomerized" ends being more stable than counterpart unprotected ends. This reduced frequency of telomere-alone signals suggests a Tax oncoprotein-mediated repression of the telomeric capping function.

The reduced frequency of MN with telomere-alone signal and the increased frequency of MN with centromere-alone signal (Fig. 5*A*) could potentially be explained mechanistically through the *de novo* generation of interstitial fragments that are not repaired by telomeric capping. To address this possibility in greater detail, we next queried for the status of TdT incorporation (*TI*) in Tax and control MN (Fig. 5*B*). Because TI of DIG-dUTP requires accessible 3′-OH DNA ends, MN negative for TI have chromosomal DNA with inaccessible 3′-OH ends. One cause of inaccessibility would be if the ends were capped by telomeric repeats with associated proteins (11, 12, 16–19). We, thus, interrogated Tax-expressing cells for frequency of MN, which were either positive (*TI*+; Fig. 5*B*, *groups 1* and *3*) or negative (*TI*−; Fig. 5*B*, *groups 2* and *4*) for incorporation of DIG-dUTP. The frequency of TI(−) MN in HeLa-Tax cells was indeed found to be significantly lower than that observed for control cells. Hence, one interpretation is that DNA breaks in control, but not Tax, cells are stabilized by telomeric capping. Consistent with this interpretation, a significant difference between control and Tax cells for Cen(+)TI(−) MN (Fig. 5*B*, *group 2*) was also observed.

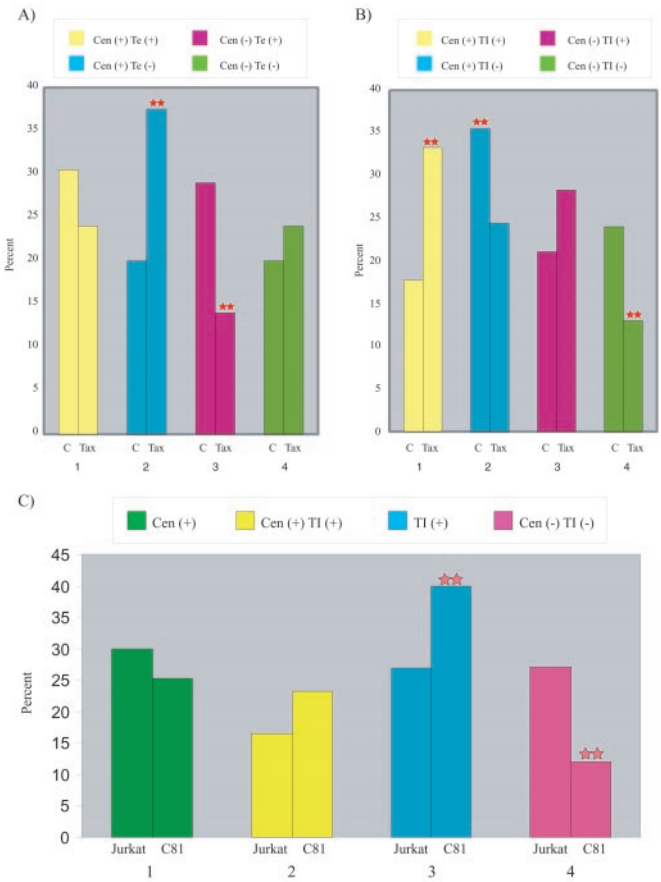

FIG. 5. **Quantitation of Tax-induced DNA damage in micronuclei from epithelial and lymphoid cells.** *A*, characterization of micronuclei in HeLa control (*C*) or HeLa-Tax-expressing (*Tax*) cells for the presence (+) or absence (−) of centromeres (*Cen*) and/or telomeres (*Te*). Centromere-specific and telomere-specific oligomeric probes were used by FISH to assess simultaneously the presence of centromeres and telomeres. Statistical significance (G test, Ref. 15): **, $p < 0.001$. *B*, frequency of micronuclei in HeLa and HeLa-Tax-expressing cells that incorporate DIG-dUTP *in situ* (*TI*). Statistical significance (G test, Ref. 15): **, $p < 0.01$. *C*, characterization of DNA by FISHI in Jurkat T-cell line and HTLV-I-transformed Tax-expressing T-cell, C8166-45, for the presence (+) or absence (−) of centromeres (*Cen*) and/or *in situ* incorporation of DIG-dUTP (*TI*). Statistical significance (G test, Ref. 15): **, $p < 0.01$.

To check that findings in epithelial cells also generally hold for T-lymphocytes (the relevant cell types for HTLV-I), we compared DNA damage (Fig. 5*C*) in Jurkat (a transformed T-cell line unrelated to HTLV-I) and HTLV-I-transformed C8166-45 cells, which express abundant amounts of Tax protein (21). In TI readouts, Tax-expressing T-cells (C8166-45) compared with Jurkat cells showed statistically significant increased frequency of TI(+) MN (Fig. 5*C*, *group 3*) and decreased frequency of Cen(−)TI(−) MN (Fig. 5*C*, *group 4*). Thus, as in HeLa cells (Fig. 5, *A* and *B*), Tax expression in T-cells increases substantially TdT-mediated DIG-dUTP incorporation, supporting a general property of this oncoprotein in abrogating intracellular telomeric capping at DNA breaks.

Here, we describe a FISHI technique to study the nature of DNA damage induced by a retroviral oncoprotein, Tax. In cells, based on the presence/absence of *in situ* incorporation at the 3′-ends of DNA fragments and on the simultaneous hybridization of centromeric/telomeric probe, we could define several classes of DNA damage, including whole chromosomes (Cen(+)Te(+)TI(−)), centric fragment (Cen(+)TI(+)), and acentric fragment (Cen(−)). A salient observation from our work is that *in situ* incorporation of DIG-dUTP correlated negatively with *in situ* hybridization by telomere-specific probe. Thus, relative ability to generate a TI signal is indicative of a telomere-free DNA break, while telomeric capping (as indicated by positive hybridization to telomere-specific probe), which is thought to stabilize breaks, adversely affects TI.

Relevant to cancer biology, our findings here help to extend generally the idea that retroviral oncogenes, like mutagens, may work commonly through heightened genomic mutability to effect transformation. Specifically, regarding HTLV-I and Tax, the current results help to explain the clastogenic changes in ATL cells not resolved by a previous study (9). Thus, FISH and FISHI findings mutually confirm and reveal that in Tax-expressing cells there is a significant decrease in the frequency of centric fragments with accessible 3′-OH DNA ends (FISHI; Fig. 5*B*, *group 2*) and a significant increase in centric fragments without telomeric signals (FISH; Fig. 5*A*, *group 2*). There was also a significant decrease in frequency of acentric fragments with telomeres (FISH; Fig. 5*A*, *group 3*) and acentric DNA without DIG-dUTP incorporation (FISHI; Fig. 5*B*, *group 4*). Collectively, these findings indicate that the increased prevalence of DNA strand breaks seen in ATL and in Tax-expressing cells is less likely explained by oncogene-induced increased incidence in strand breakages as by oncogene-mediated suppression of a DNA end-stabilizing mechanism (*i.e.* telomeric capping). This study provides the first detailed characterization of DNA breaks induced by a viral oncoportein. Our conclusions add to the growing body of evidence of an operationally defined *mutator* phenotype for Tax-expressing cells (22–25). Future investigations will help to shed further light on the ensemble of cellular factors impinged upon by Tax in generating this phenotype.

Acknowledgments—We thank H. Iha, T. Kasai, K. Kibler, Y. Iwanaga, Y. Wu, and V. Yedavalli for critical readings of manuscript and L. Lin for preparation of manuscript and figures.

REFERENCES

1. Li, R., Sonik, A., Stindl, R., Rasnick, D., and Duesberg, P. (2000) *Proc. Natl. Acad. Sci. U. S. A.* **97,** 3236–3241
2. Perucho, M. (1996) *Biol. Chem.* **377,** 675–684
3. Loeb, K. R., and Loeb, L. A. (2000) *Carcinogenesis* **21,** 379–385
4. Kibler, K. V., and Jeang, K. T. (1999) *J. Natl. Cancer Inst.* **91,** 903–904
5. Majone, F., Semmes, O. J., and Jeang, K. T. (1993) *Virology* **193,** 456–459
6. Semmes, O. J., Majone, F., Cantemir, C., Turchetto, L., Hjelle, B., and Jeang, K. T. (1996) *Virology* **217,** 373–379
7. Majone, F., Brunetti, R., Fumagalli, O., Gabriele, M., and Levis, A. G. (1990) *Mutat. Res.* **224,** 147–151
8. Majone, F., Tonetto, S., Soligo, C., and Panozzo, M. (1992) *Teratog. Carcinog. Mutage.* **12,** 155–166
9. Jin, D. Y., Spencer, F., and Jeang, K. T. (1998) *Cell* **93,** 1–20
10. Driller, L., Wellinger, R. J., Larrivee, M., Kremmer, E., Jaklin, S., and Feldmann, H. (2000) *J. Biol. Chem.* **275,** 24921–24927
11. Martin, S. G., Laroche, T., Suka, N., Grunstein, M., and Gasser, S. M. (1999) *Cell* **97,** 621–633
12. Matsumoto, T., Fukui, K., Niwa, O., Sugawara, N., Szostak, J. W., and Yanagida, M. (1987) *Mol. Cell. Biol.* **7,** 4424–4430
13. Matera, A. G., and Ward, D. C. (1993) *Hum. Mol. Genet.* **1,** 535–539
14. Miller, M., and Nusse, M. (1993) *Mutagenesis* **8,** 35–41
15. Sokal, P., and Rohlf, F. J. (1991) *Biometry*, Freeman, San Francisco, CA
16. Pologe, L. G., and Ravrech, J. W. (1988) *Cell* **55,** 869–874
17. Gilley, D., Preer, J. R., Jr., Aufderheide, K. J., and Polisky, B. (1988) *Mol. Cell. Biol.* **8,** 4765–4772
18. Kamper, J., Meinhardt, F., Gunge, N., and Esser, K. (1989) *Mol. Cell. Biol.* **9,** 3931–3937
19. Yu, G. L., and Blackburn, E. H. (1991) *Cell* **67,** 823–832
20. Fiumicino, S., Martinelli, S., Colussi, C., Aquilina, G., Leonetti, C., Crescenzi, M., and Bignami, M. (2000) *Int. J. Cancer* **85,** 590–596
21. Jeang, K. T., Derse, D., Matocha, M., and Sharma, O. (1997) *J. Virol.* **71,** 6277–6278
22. Jeang, K. T., Widen, S. G., Semmes, O. J., and Wilson, S. H. (1990) *Science* **247,** 1082–1084
23. Kao, S. Y., and Marriott, S. J. (1999) *J. Virol.* **73,** 4299–4304
24. Miyake, H., Suzuki, T., Hirai, H., and Yoshida, M. (1999) *Virology* **253,** 155–161
25. Philpott, S. M., and Buehring, G. C. (1999) *J. Natl. Cancer Inst.* **91,** 933–942